Marine Geophysical Researches (2006)
DOI 10.1007/s11001-005-5999-0

Seabed characterization through a range of high-resolution acoustic systems – a case study offshore Oman

Magdalena Szuman[1,2,*], Christian Berndt[1], Colin Jacobs[1] & Angus Best[1]
[1]*Challenger Division for Seafloor Processes, National Oceanography Centre, University of Southampton, Waterfront Campus, European Way, SO14 3ZH, Southampton, UK*
[2]*Department of Geology and Petroleum Geology, University of Aberdeen, Kings College, AB24 3UE, Aberdeen, UK*
**Corresponding author (Phone: +44-0-1224-372425; Fax: +44-0-1224-372785; E-mail: m.szuman@ abdn. ac.uk)*

Received 25 April 2005; accepted 15 December 2005

Key words: 3.5 kHz sediment profiler, acoustic characterization, backscatter, bioturbation, deep-tow CHIRP, EM12 multibeam, Oman

Abstract

This study uses three acoustic instruments (different in their operating frequencies, 13, 3.5, and 6–10 kHz, and deployment type, hull-mounted, surface-towed and deep-towed) to investigate and characterize the acoustic response of seafloor NE of Oman in a frequency-independent manner. High-resolution control was achieved by having selected areas of our acoustic transects ground-truthed by sampling and/or sea-floor photography. On the regional scale, the greatest degree of change in backscatter amplitude was correlated with major changes of seabed morphology and lithology. However, small-scale roughness had the biggest effect on amplitude on the local scale, i.e. within each area of specific seafloor type. The study also shows that seafloor reflection amplitude changes are far more easily detected by deep-towed instrument than by surface-towed or hull-mounted systems. Whilst there are significant changes in bioturbation types and density along the transects, the suite of instruments deployed was not able to pick up the effect of the bioturbation on acoustic signals.

Introduction

In recent years, seabed mapping has become a common tool for geological and geophysical exploration. Sidescan sonar and multibeam echo sounders are used to obtain high-resolution surface data, and deep-tow, high-resolution reflection profilers provide subsurface information (Savoye et al., 1995; Nouze et al., 1997; Gracia et al., 1998; Briais et al., 2000; Nealon et al., 2002). Many studies employ a combination of techniques, e.g. multibeam and sidescan sonars images, to map the surface sediment distribution and high resolution seismic profiles to extrapolate this distribution into the sub-surface (Scheirer et al., 2000; Schuur Duncan and Goff, 2001; Schuur Duncan et al., 2000; Veeken and Da Silva, 2004; Zitter et al., 2005).

In general, the methods used in marine geosciences can be divided into two major groups. The first includes sidescan sonars and multibeam swath bathymetry. The use of high frequency (12 kHz) sonars may allow the physical properties of the seafloor to be derived at sufficient resolution to distinguish both lateral and vertical changes that are related to sedimentary facies and possibly even bio-geochemical alteration. Sediment classification by sonar is based on inversion of echo returns to estimate the acoustic impedance of the seafloor. Empirical relationships between seafloor impedance and sediment physical properties are then used to map seafloor physical properties such as porosity, bulk density, sand and gravel fraction, mean grain size, and geoacoustic properties such as sound speed and attenuation. Classification of seafloor lithology is based on the ability to distinguish between different seabed reflection amplitudes, while seabed characterization relies on the inversion or interpretation of the measured

amplitudes in terms of the physical properties of interest (Richardson and Briggs, 1993). Most of these studies were confined to a single acoustic source and given the different acoustic response for different geologic environments it is difficult to generalize these findings.

The second group covers a broad range of different seismic techniques which are used to probe the sub-surface and to investigate their geological history and evolution. Echo sounding and seismic reflection profiles have been widely used for mapping deep-sea morphology and for sediment classification over the last 50 years (e.g. Milliman, 1988; Leblanc et al., 1992; Kim et al., 2003). Early morphological charts, often derived from 12 kHz echo soundings, concentrated on seafloor topography (Heezen et al., 1959). Low frequency seabed profilers (e.g., the 3.5 kHz) were developed in the late 1960s to image beneath the seabed and have been widely used. The greater acoustic penetration of these systems enabled not only the acoustic reflection characteristics of the seafloor to be determined, but also those of the uppermost sediments down to typically from 5 to 50 m beneath the seabed.

Data presented in this study was collected during a multi-disciplinary research cruise offshore Oman from 22 November to 20 December 2002 on the RRS Charles Darwin (Jacobs, 2003). The aim of the cruise was to integrate benthic biology and marine geology/geophysics studies to gain insight into the bio-geoacoustic properties of the seafloor.

The first objective of this paper is to determine if a compilation of different acoustic remote sensing methods (c.f. different operating frequencies and thus responses) over the same area can better characterize the seabed than a single method. Secondly, we investigate the strengths and weaknesses of different acoustic methods to estimate seabed properties. To this end we compare the response of three different acoustic systems to groundtruthing that we obtained by seabed photography and sediment cores. The systems that we deployed simultaneously offshore Oman included: a 3.5 kHz surface-towed sediment profiler, backscatter information from a hull-mounted, Simrad EM12 multibeam swath mapping system; and Southampton Oceanography Centre's new deep-towed CHIRP reflection profiler system, which we analyze in more detail. Finally, we assess the feasibility of detecting biologically influenced changes in seafloor properties using remote acoustic methods.

Geological background

The Gulf of Oman is a roughly triangular basin bordered by Oman to the south west and Iran and Pakistan to the north. The Straits of Hormuz connect it to the Persian Gulf in the northwest. The basin is separated from the eastern part of the Arabian Sea to the south by the 420 km long north-east-trending Murray Ridge. Despite many studies carried out in this area (Shimmield et al., 1990; Gage and Levin, 2000; Meadows et al., 2000) there is not much published information about the north east Oman Margin. According to Uchupi et al. (2002), the upper slope and outer shelf edge are irregular and the mid-upper slope is smooth. However, the swath bathymetry collected with the EM12 multibeam swath mapping system during our cruise shows for the first time a series of deeply incised canyons along the entire margin (Figure 1).

The basin scale circulation of the Arabian Sea is governed by the seasonally reversing monsoon cycle consisting of Fall intermonsoon from mid-September to October, Northeast monsoon from November to February, Spring inter-monsoon from mid-February to May. From June to mid-September Southwest monsoon brings into the area the biggest amount of the sediment deposited in the region during the year. It can exceed 80×10^6 m^3 s^{-1} over the 4 months of the SW Monsoon around Cape al Hadd (Leetmaa et al., 1982). The shelf area west of the Murray Ridge is covered by terrigenous sediments with exposure of bedrocks. The terrigenous sediments are predominantly mud with sands, muddy sands and sandy mud (Uchupi et al., 2002). The sediments record a variety of organic carbon-rich, biogenic silica-rich and biogenic carbonate-rich facies which are deposited under upwelling (Shimmield et al., 1990).

Methods

Using EM12 multibeam swath mapping system, we first recorded a high-frequency (13 kHz), backscatter and bathymetry data set along the Oman Margin. Swath width was approximately 3.5 times the water depth with an usable depth range

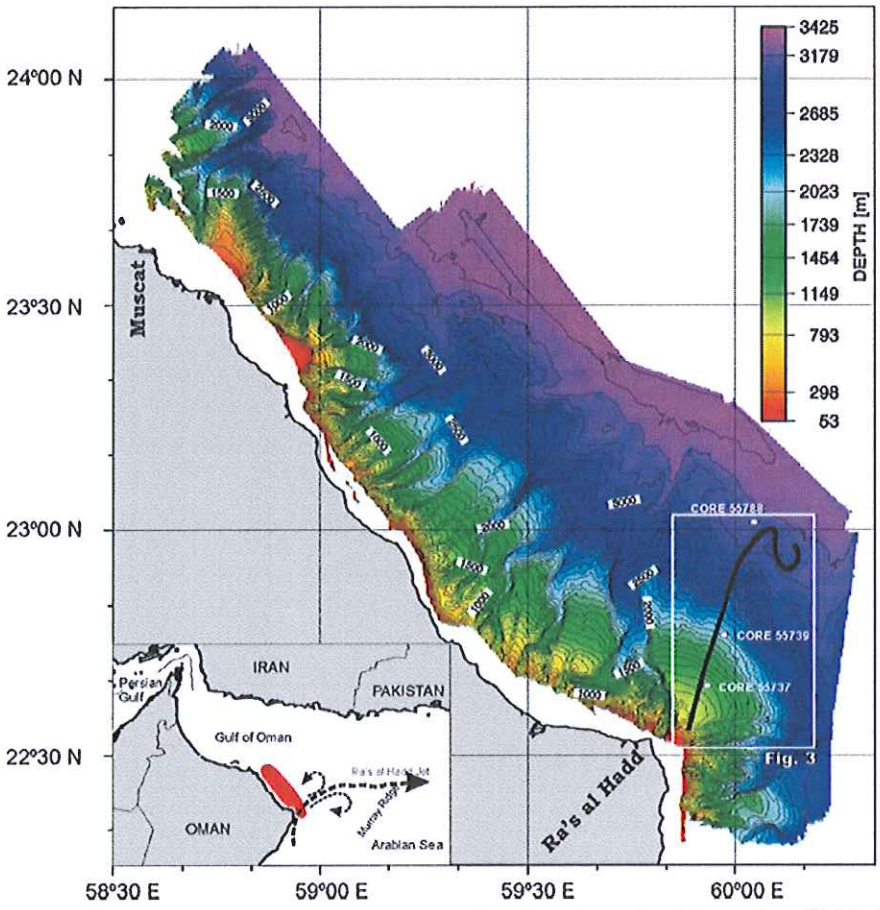

Figure 1. Multibeam bathymetry chart of the NE Oman margin collected during cruise CD143. The solid black line shows the transect used for the acoustic data analysis, dashed black line–dominant current direction during Southwest monsoon, white box–location of Figure 3.

between 50 and 3000 m. The insonification angle was 150° for 162 beams. These parameters result in a footprint for a single beam between 15 m in shallow water and up to 70 m in the deepest areas (Hammerstad et al., 1993) (for more technical details see Table 1). Survey lines were generally maintained parallel to the shore to maximize data coverage and to facilitate mosaicing of the swath data to generate bathymetric and acoustic backscatter charts of the survey area. The backscatter mosaic with a 20 m resolution was draped over the bathymetry to produce a 3D seabed image which enabled a suitable transect to be located for this study.

Table 1. Technical specification for EM12 multibeam swath mapping system, deep-towed CHIRP and 3.5 kHz sediment profiler.

	Frequency	Vertical resolution	Horizontal resolution	Penetration	Deployment type
EM12 multibeam swath mapping system	13 kHz	≈0.02 m	≈6 m for 50 m water depth ≈350 m for 3000 m water depth	<5 m	Hull-mounted
CHIRP	6–10 kHz	≈0.18 m	≈45 m	≈22 m	Deep-towed
3.5 kHz Sediment profiler	3.5 kHz	≈0.3 m	≈22 m for 50 m water depth ≈1300 m for 3000 m water depth	<100 m	Surface-towed

Digital data from the 3.5 kHz sediment profiler and the 6–10 kHz deep-towed CHIRP (Mini Profiler Vehicle) echo-sounder system were simultaneously collected along the transect (Figure 1). Raw data were converted into SEG-Y format before processing with the commercial seismic data processing software ProMAX. The processing included frequency filtering and deconvolution. The available navigation accuracy excludes the option of migration because the very high frequency would require static corrections that are not achievable with the present navigation accuracy.

The Mini Profiler Vehicle is a deep-towed, normal-incidence, acoustic reflection, sub-bottom CHIRP profiling system using frequencies between 6 and 10 kHz and a beam angle of 25°. By 'flying' the deep-towed CHIRP at a near-constant altitude above the seafloor (200–500 m), high-resolution sub-seabed seismic reflection data were obtained with a penetration of up to 30 ms two-way travel time (TWT), approximating to 22 m, assuming a water velocity of 1500 ms^{-1}. A draw back to this system is that the deep-towed CHIRP can only be towed at speeds <2 knots, much slower than conventional surface-towed sediment profilers such as the 3.5 kHz. During the cruise the deep-towed CHIRP was deployed twice and over 150 km of shallow-penetration (up to 20 m) acoustic data were collected during that time (Figure 1). The recorded data are characterized by high levels of noise, which might result from electrical induction into the long deck cable.

The 3.5 kHz sediment profiler comprises a combined transceiver and correlator unit, a logging and display unit, the winch and deployment davit and the 3.5 kHz transducer fish, which has a beam angle of 45°. The 3.5 kHz sediment profiler record reflects the geometry and thickness of the upper few 10s of meters of sediment. The transducer fish gave good results at ship speeds up to 8 knots; above this, noise dominated the recorded data. During the cruise approximately 4000 km of high-resolution profiles were collected from the area between Muscat and Ra's al Hadd.

To ground truth our acoustic observations we also deployed the Seafloor High Resolution Imaging Platform (SHRIMP), which is Southampton Oceanography Centre's deep-towed video and camera imaging system. All signals and data to and from the vehicle are sent via a fiber-optic link. Visual contact is made when the vehicle is within 10 m of the seabed. A 6 kg lead weight on a 3 m tether is used as a visual altimeter and guides the pilot of the vehicle to keep the optimum height of 3 m above the seafloor. Absolute altitude is measured by a very high frequency echo-sounder. SHRIMP was deployed seven times along the transect, providing several hours of seabed imagery data. The greatest depth of the deployment was 3300 m and the shallowest was 290 m (Figure 1).

During the cruise, a series of gravity Kastenlot cores were retrieved with a Hydrowerkstätten system. The corer can be used with 1, 2, or 3 m long square-section barrels which have a cross-section of 150×150 mm. Three cores were taken along the transect covering the top part of the upper slope, mid-slope and the continental rise.

Observations

Three gravity cores 55737, 55739 and 55788 were collected along the transect (Figure 1). The geological core descriptions are summarized in Figure 2 and confirm that the sediments in this area are mostly mud and clay with a small amount of sandy mud.

Preliminary onboard interpretation of EM12 multibeam swath mapping system data was used as a guide to locate the appropriate regions for deployment of the deep-towed CHIRP for seafloor characterization along the transect. We chose the transect north east of the Ra's al Hadd to focus upon for this study (Figure 3) as it covers the largest number of different environments, i.e. the upper slope, middle slope and continental rise areas.

The upper slope

The upper slope includes type *Area A* (Figure 3) and covers the seabed from 400 to 1000 m water depth. The shallowest part (400–500 m) is mostly flat. Detailed analysis of the echo-sounder bathymetric profile shows small-scale (the smallest 1m deep) topography in this region. SHRIMP photographs and video show that it is caused by outcropping rocks – probably bedrock outcrops (Figure 4c). Between 500 and 900 m water depth the slope is steepest (30°) before the slope

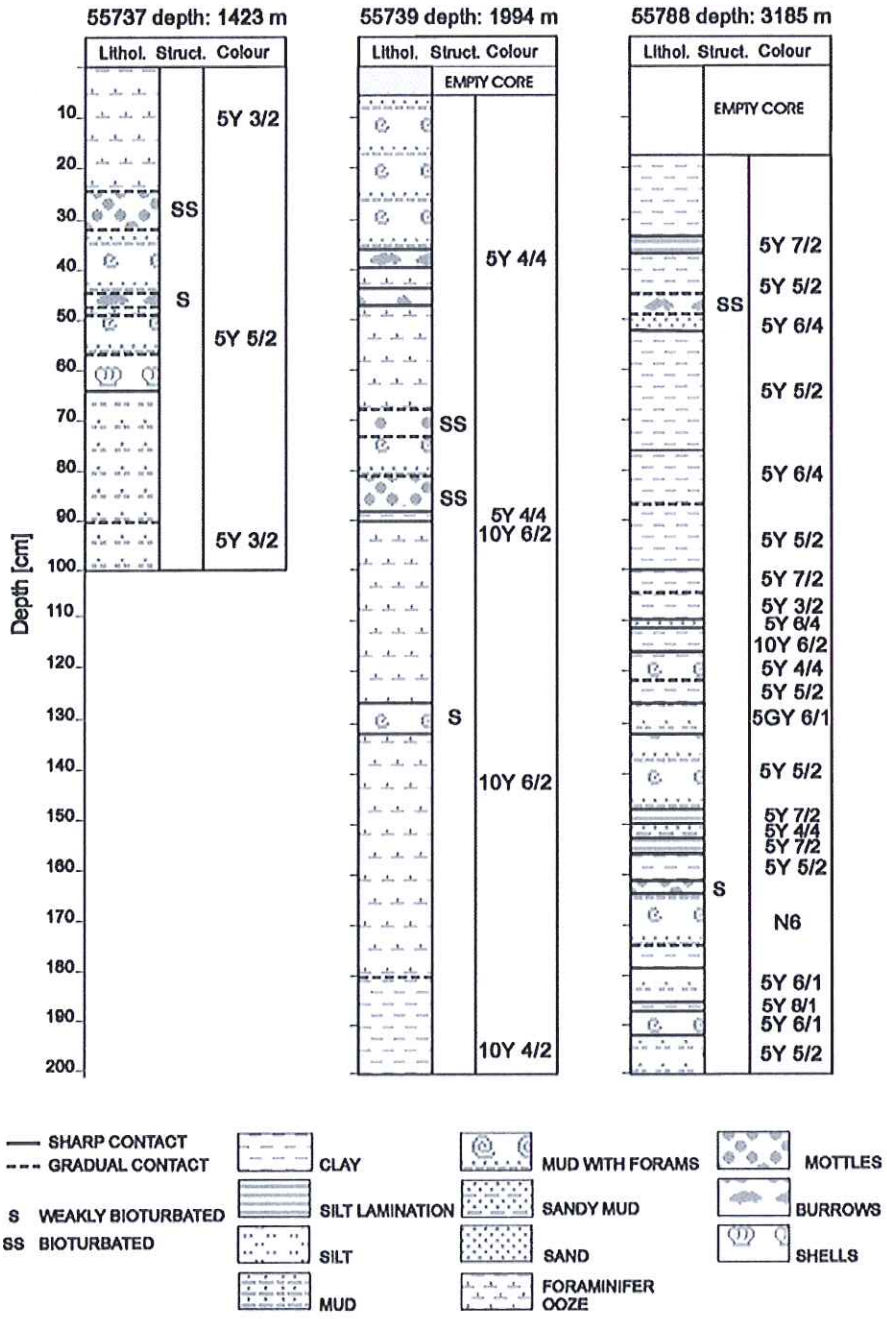

Figure 2. Geological core descriptions for the cores shown in Figure 1. Lithol., = Lithology; Struct. = Structure.

continues further down as a gently dipping, mostly smooth surface (Figure 4a, b).

The upper slope has higher EM12 multibeam swath mapping system and 3.5 kHz sediment profiler data reflection amplitudes than the rest of the transect (Figure 5c, b). But whereas the 3.5 kHz sediment profiler seabed reflection amplitudes are characterized by a maximum at the base of the upper slope and a reduction with decreasing water depth, on the EM12 multibeam swath

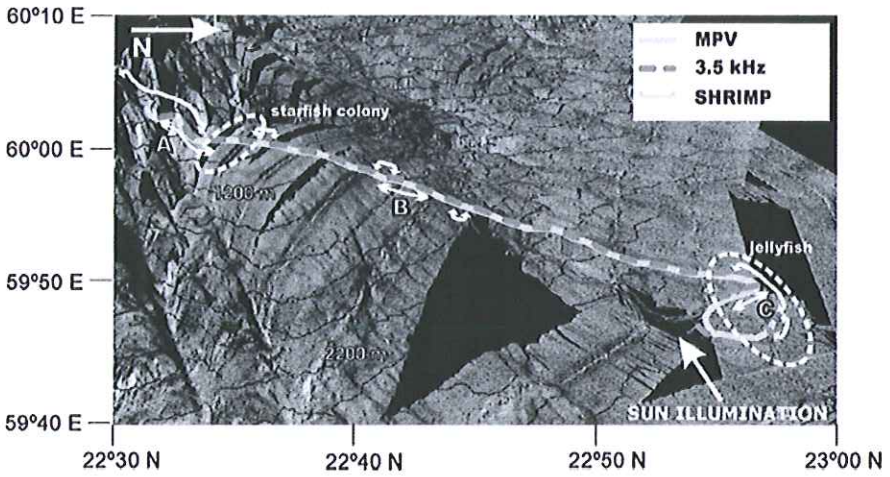

Figure 3. Backscatter data in the vicinity of the southern transect off Ra's al Hadd that was used for the acoustic analyses. White arrows indicate type localities shown in Figures 4, 6 and 7. Solid black lines indicate 200 m contours. Dark, low backscatter; Light, high backscatter.

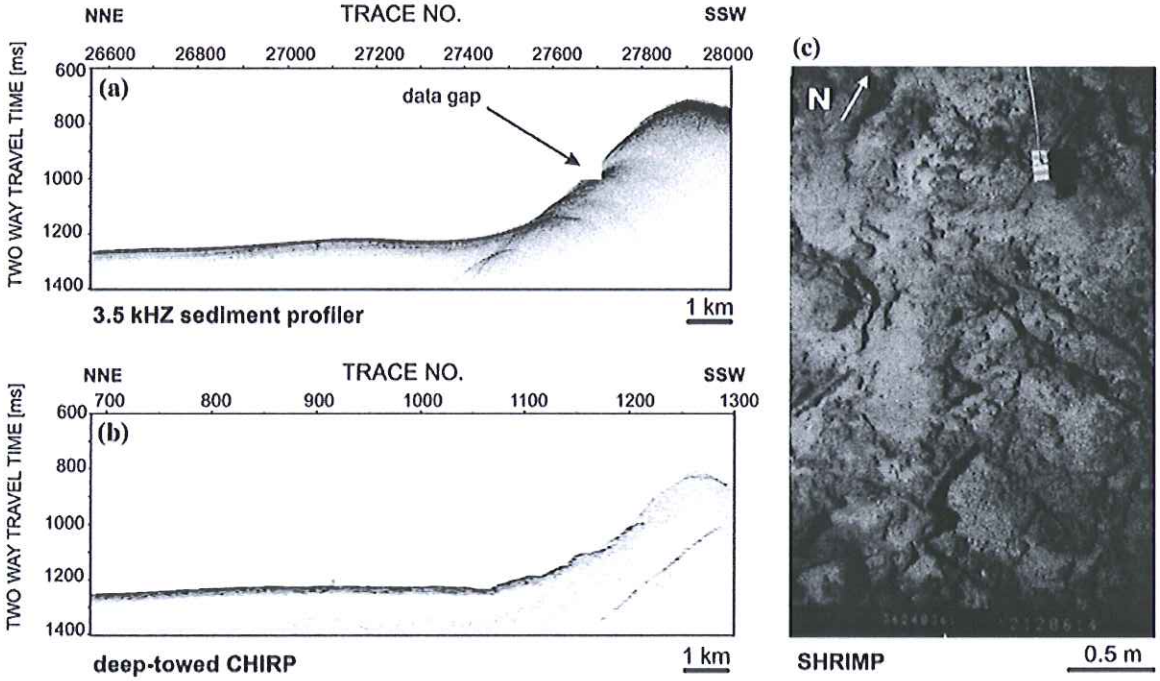

Figure 4. (a) Seabed reflection amplitude from the 3.5 kHz sediment profiler, (b) deep-towed CHIRP, and (c) SHRIMP seabed photograph obtained upper slope (*Area A* on Figure 3).

mapping system, the amplitude constantly increases from the bottom of the upper slope and rises by approximately 25%, reaching its maximum in the shallowest part covering *Area A*. An increase in reflectivity can be observed at the shallowest part of the survey on the deep-towed CHIRP data (Figure 5c), but it is not as pronounced as seen in the EM12 multibeam swath mapping and 3.5 kHz sediment profiler data. Whereas the 3.5 kHz sediment profiler data show many diffraction

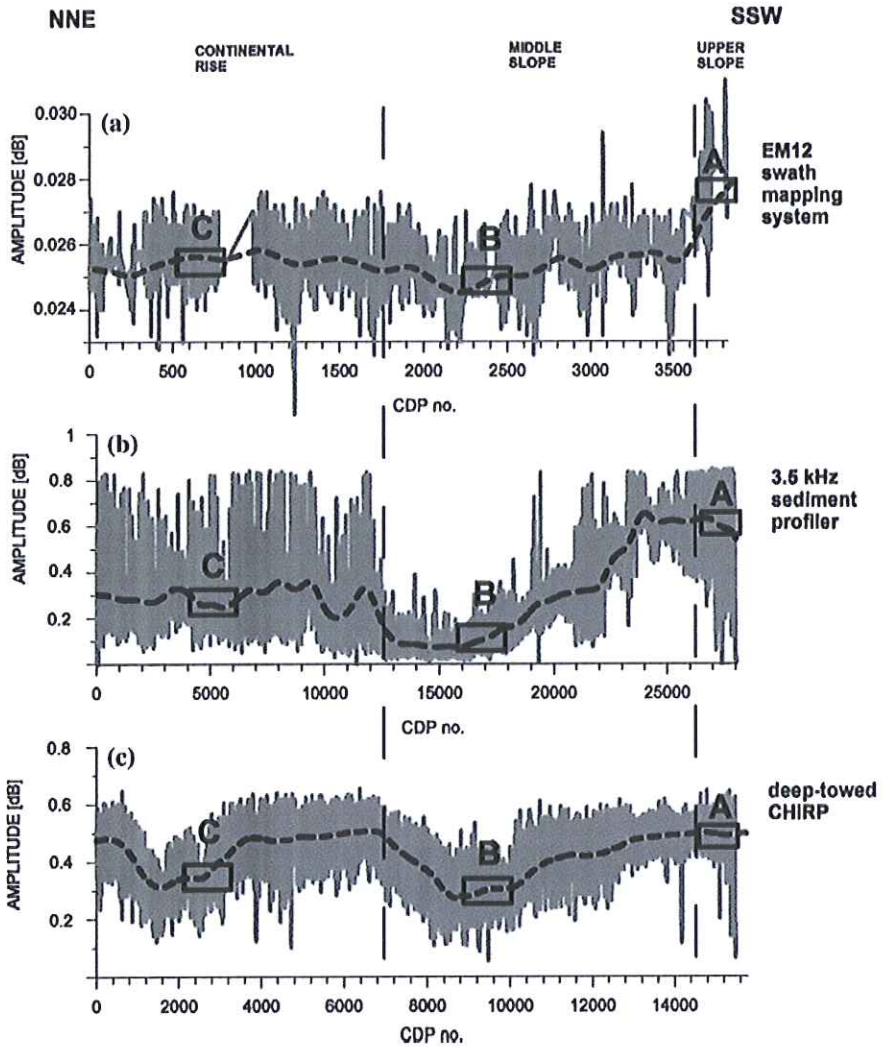

Figure 5. Seabed amplitudes for the three acoustic sources along the transect shown in Figures 1 and 3.

hyperbolas, the deep-towed CHIRP data clearly image the rough surface.

The middle slope

The middle slope includes Area B (Figure 3) and stretches from 1000 m down to 3000 m water depth. Between 1000 and 1200 m, the seabed has a smooth surface, similar to Area A. From 1200 m the seabed slopes gently (approximately 10°; Figure 6a, b). As water depth increases, the slope surface becomes more undulated with a series of shallow channels parallel to each other and perpendicular to the shore (Figure 3). The SHRIMP pilots guide weight on the video shows a plume of sediment being washed from the surface of the weight after it hit the seafloor. Because these sediments suspend this shows that they are medium- to fine-grained (Figure 6c). Analysis of two gravity cores collected along slope area, i.e. 55737 and 55739 (Figure 1) confirmed that the sediment in this area consists of pelagic mud and muddy ooze.

The EM12 multibeam swath mapping data do not show large amplitude changes within the middle slope area (Figure 5a). However, one

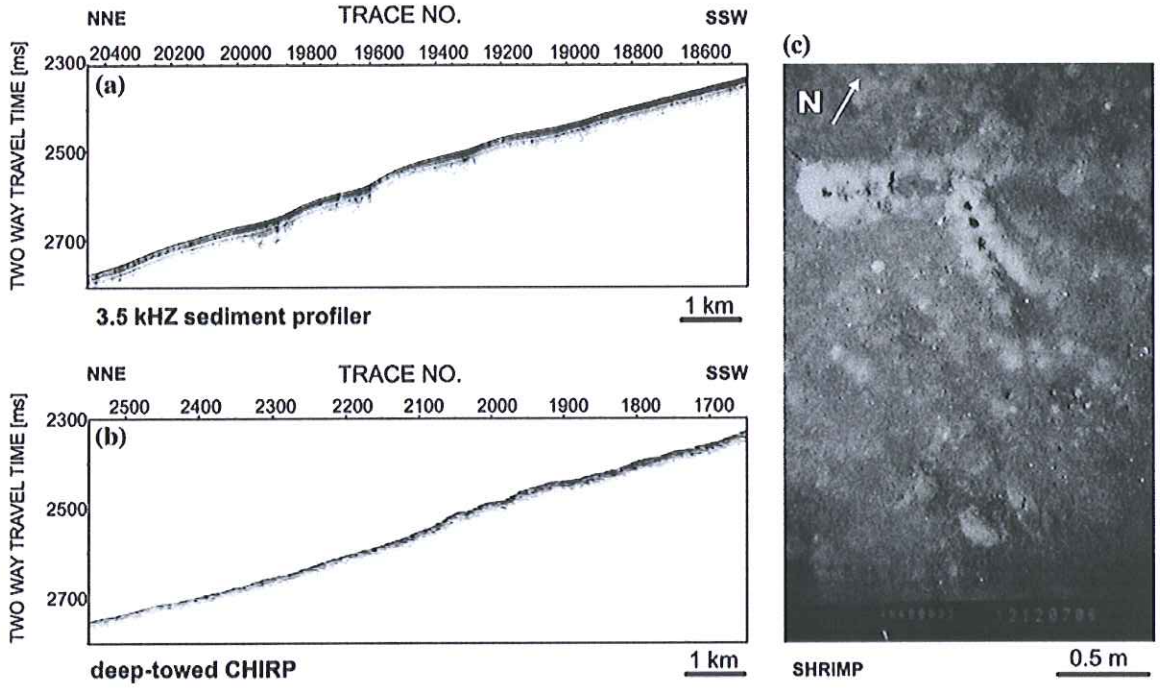

Figure 6. (a) Seabed reflection amplitude from the 3.5 kHz sediment profiler, (b) deep-towed CHIRP and (c) SHRIMP seabed photograph obtained on the middle slope (*Area B* on Figure 3).

major decrease in seabed reflectivity exists on the bottom part of the slope (CDP no 2000–2400, Figure 5a) in *Area B*. In contrast, the 3.5 kHz sediment profiler amplitude shows the biggest changes in the slope area compared for the entire survey. After a maximum at the top of the region (CDP no 2400–2600, Figure 5b) amplitude values decrease by 600% reaching their minimum (0.1 dB) at the bottom (CDP no 1300–1600, Figure 5b). The deep-towed CHIRP data show a significant amplitude trough (Figure 5c) at the bottom part of the slope including *Area B* (CDP no 7000–10,800). Apart from this decrease, the amplitudes constantly increase without any major peaks along the study area.

The continental rise

The continental rise includes *Area C* (Figure 3). It is covered by various terrain undulations (Figure 7a, b), which may be caused by small scale sediment slumping. These undulations can have as much as 25 m relief estimated from the deep-towed CHIRP profile. SHRIMP photographs and video suggest that the seabed is composed of fine-grained sediments (Figure 7c). Gravity core no 55788 was collected in the continental rise area and analysis verified its composition as mixture of clay and silt with a small percentage of sand and sandy mud (Figure 2). Over a large area, the seafloor is covered by an approximately 1 cm-thick layer of dead jellyfish *Crambionella orsini* (Billett et al., 2003).

There are no significant seabed backscatter amplitude variations on the EM12 multibeam swath mapping profile along the continental rise (Figure 5a). The 3.5 kHz sediment profiler seabed amplitudes show much bigger variations in this area. There are two troughs in the profile over small regions (CDP no 400–600 and 9500–11,500) including *Area C* (Figure 5b). On the deep-towed CHIRP profile there is one major decrease in seabed reflection amplitude covering almost half of the continental rise region, including *Area C* (CDP 400–3600). The second part of the area is characterized by a constant amplitude rise of approximately 60% in comparison to the above mentioned trough.

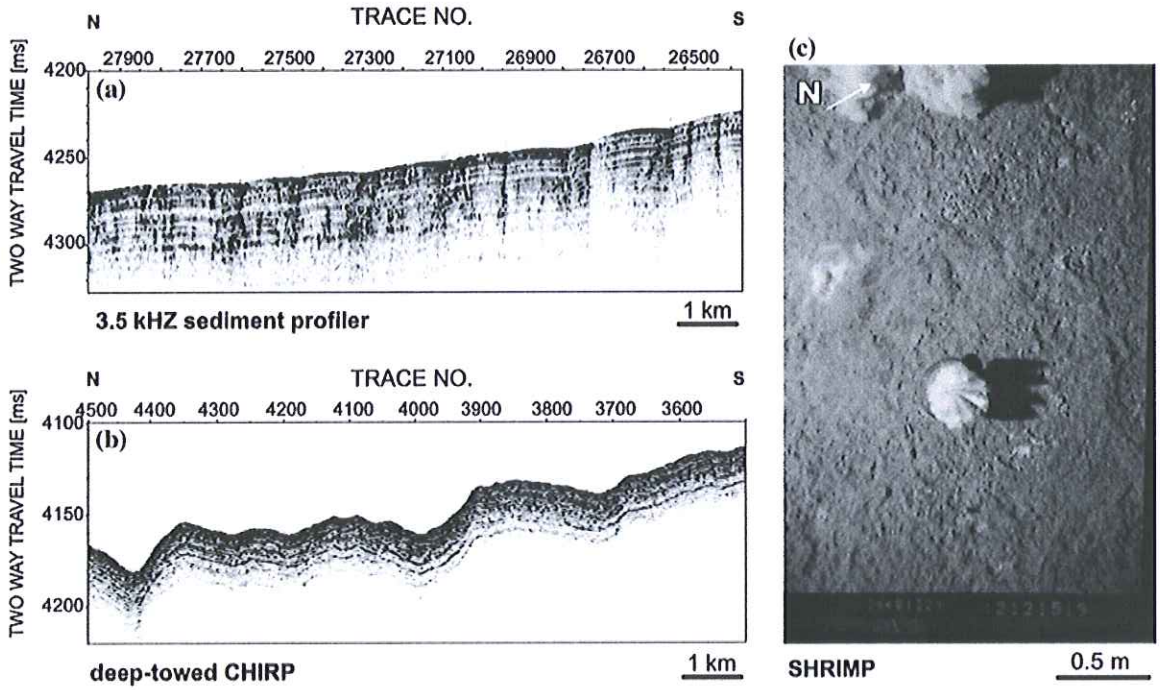

Figure 7. (a) Seabed reflection amplitude from the 3.5 kHz sediment profiler, (b) deep-towed CHIRP and (c) SHRIMP seabed photograph obtained for part of the continental rise (*Area C* on Figure 3).

Discussion

Suitability of different acoustic methods for seabed characterization

Seafloor character from SHRIMP imagery

According to the SHRIMP images the study area can be divided into two separate regions with different sediment type. The top part of the upper slope consists of a hard seabed with outcropping rocks. The second area comprises the lower section of the upper slope, the entire slope, and continental rise area. Sediment cores taken along the transect show that this lower part is covered with clayey mud with a small percentage of sand (Figure 2).

EM12 multibeam swath mapping system's backscatter information

On the top of the upper slope the seabed backscatter amplitude rises by about 25%, corresponding to the bedrock observed on the SHRIMP photographs. The EM12 multibeam swath mapping data do not show large amplitude changes along the slope and continental rise areas. However, two decreases in reflectivity values in the continental rise (CDP no. 100–200) and in the middle-slope (CDP no. 2000–2500) can be discerned (Figure 5a). Given its footprint which varies from 15 m radius in the shallow water to 70 m for a single beam with water depth around 3000 m, its large lateral coverage, and the simultaneous collection of topographic information, the EM12 multibeam swath mapping system is a very efficient tool for determining regional variations in backscatter. However its resolution is three to ten times lower than modern high-frequency side-scan sonar systems and lower than deep-towed seismic systems. This lack of resolution makes it far less useful for deciphering sediment transport processes on anything but a course scale (Keeton and Searle, 1996; Cowls and Fogg, 2000).

3.5 kHz sediment profiler information

The seabed reflection amplitude profile recorded by the 3.5 kHz sediment profiler has its maximum in the upper slope area. A general decrease in amplitude can be observed for the entire slope. Moreover, there is a significant amplitude decrease from the major trend located in the middle-slope.

Amplitude values are mostly constant within the continental rise section. In this area variations do not exceed 15% of the average value. Because this amplitude decrease is also observed in the deep-towed CHIRP data and also but to a lesser extent in the EM12 multibeam swath mapping data, and because there are no obvious wave propagation effects causing this amplitude decrease, we conclude that it is caused by a real change in seabed reflectivity. Possibly it represents a preferential deposition centre, caused by lower bottom current velocities such as in slope basins in accretionary prisms (Underwood and Moor, 1995). The large acoustic seafloor footprint of the 3.5 kHz sediment profiler (approximately 160 m radius in 400 m water depth and 1250 m in 3000 m) reduces the spatial resolution of the system particularly in great water depths and gives rise to diffraction hyperbolas in areas of significant topography (Figure 8). This effect results in the system's decreased ability to detect small-scale lateral changes in sediment type along the continental rise. The 3.5 kHz sediment profiler seabed reflection amplitudes show a strong correlation with towing height, i.e. water depth, indicating that spherical divergence is the primary cause of amplitude variation. Therefore, meaningful geological interpretation of the absolute amplitudes of the 3.5 kHz sediment profiler requires accurate amplitude-travel time correction. However, even with this correction the system only allows seabed characterization on a 100–200 m scale at water depths more than 1000 m.

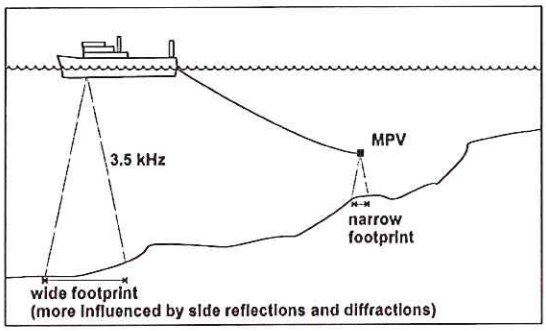

Figure 8. Schematic of 3.5 kHz sediment profiler and MPV data acquisition showing relative seabed footprint sizes.

Deep-towed CHIRP seabed characterization

To assess the suitability of the deep-towed CHIRP for seabed characterization it is necessary to understand better the correlation between towing height of the CHIRP and the effect of wave propagation phenomena on the recorded amplitudes. Comparison of the deep-towed CHIRP data sets from upper slope, middle-slope and continental rise (Figure 3 areas A, B and C) suggests that the amplitude values do not change significantly when the towing height is less than 400 ms (TWT) corresponding to approximately 300 m if you assume 1500 m/s as sound speed in the water (Figures 9–11). The top part of the upper slope is an exception to this rule. Here a large amplitude decrease can be observed for the towing height as low as 140 ms (TWT) (Figure 9a, b). The decrease in amplitude in the other areas like the top of the upper slope and at the bottom of the slope, still with towing heights below 400 ms (TWT) (300 m) (Figures 9a, b and 10a, b) suggests that both sediment lithology and seabed topography have a strong effect on the reflectivity values. As described above, the top part of the upper slope area is composed of rocks, whilst the bottom part has a smooth surface. The morphological difference between these regions is reflected in their seabed reflection amplitudes.

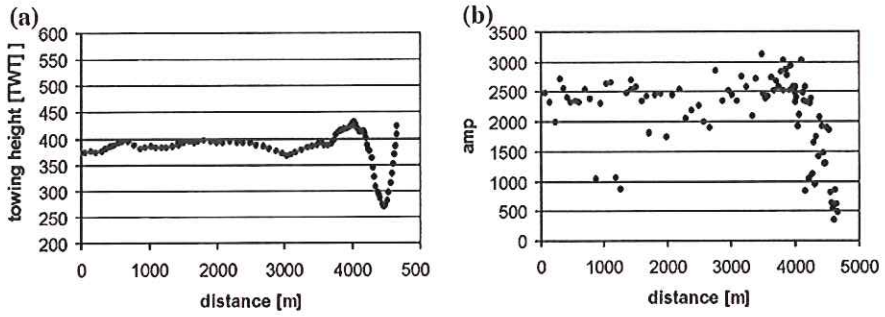

Figure 9. The relationship between towing height and seabed reflection amplitude for the upper slope.

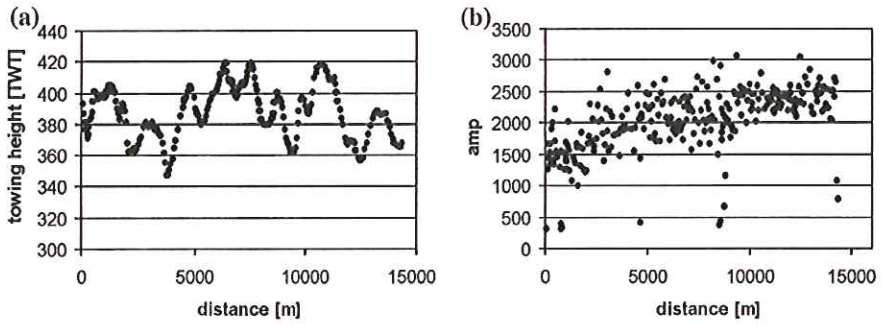

Figure 10. The relationship between towing height and seabed reflection amplitude for middle slope.

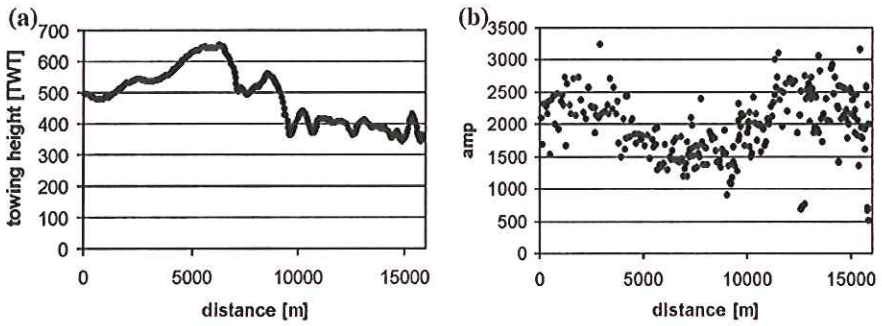

Figure 11. The relationship between towing height and seabed reflection amplitude for continental rise.

If towed at the normal operational towing depth range of 330–400 ms (TWT) or 250–300 m above the seabed, the deep-towed CHIRP amplitude profile does not show a strong effect of diffraction and spherical divergence (Figure 12a, b), in contrast to the 3.5 kHz sediment profiler. Because the deep-towed CHIRP can be operated in a way that largely excludes these effects, this instrument is able to image the acoustical properties of the seabed due to changes in lithology and small-scale topography.

Comparison of the results of three systems with their advantages and drawbacks

The most significant change in seabed reflectivity deduced from the EM12 multibeam swath mapping reflectivity data is the increase of backscatter from the upper slope. The detailed investigation of amplitude variations shows that the EM12 multibeam swath mapping system delivers relatively high-resolution backscatter information (in comparison to 3.5 kHz sediment profile) with large spatial coverage, which is very suitable for regional seabed surface characterization. However, because it is hull-mounted, its lateral resolution RMS accuracy varies between 0.2% of depth (from vertical up to 45°) and 0.5% of depth (between 60° and 70°) and due to its nature it lacks subsurface information.

The most significant change in seabed reflectivity from the upper slope is also deduced by 3.5 kHz sediment profiler. However, in comparison with deep-towed CHIRP this system is not well suited for detailed seabed characterization especially in deep water areas. Due to the wide footprint it is only useful for regional studies. It can however provide subsurface information.

The increase of backscatter from the upper slope is not seen in the deep-towed CHIRP data. We propose that the lack of major amplitude variations reflects the influence of small-scale terrain undulations on the deep-towed CHIRP data. The small-scale seabed undulations strongly increase scattering of the wave energy and this is more easily detected by the high spatial resolution of the deep-towed CHIRP system than by the conventional 3.5 kHz sediment profiler. Unfortunately, the resolution of the acquired bathymetry

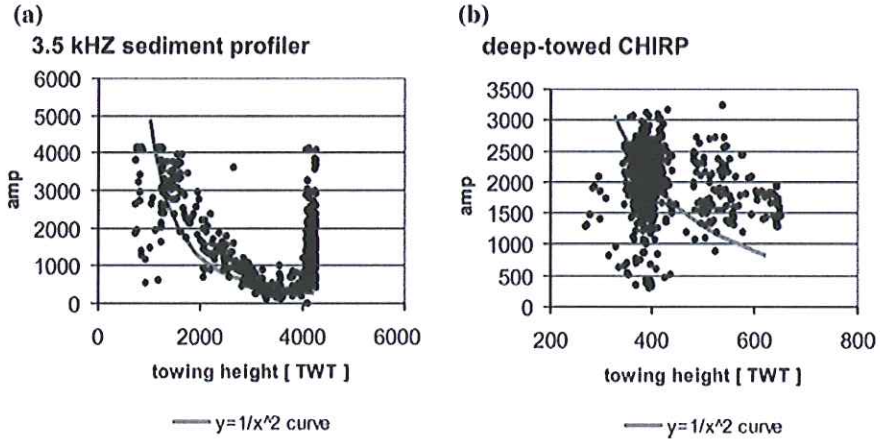

Figure 12. The relationship between towing height and seabed reflection amplitude for 3.5 kHz sediment profiler (a) and deep-towed CHIRP (b).

data is not sufficient to calculate the statistical description of the seabed roughness, which would allow analytical quantification of the rough surface effect on backscatter (Thorne and Pace, 1984).

The deep-towed CHIRP provides seabed reflectivity data with high lateral resolution and high sensitivity because it is towed at depth. Due to its penetration it provides sub-seabed information, which is not of very high fidelity at its current development stage. Its observed dependence on seabed roughness along the upper slope gives useful additional information if the system is used in combination with another, e.g. the EM12 multibeam swath mapping system. In this case it allows determining both reflectivity and roughness of the seabed. On the other hand it makes the data more difficult to interpret if the deep-towed CHIRP system is used on its own. In this case both the mean amplitudes and their deviation have to be used to arrive at a meaningful interpretation.

Suitability of different acoustic methods for detecting biological changes on the seafloor

According to the SHRIMP images, there are different ecosystems along the transect.

At water depths of up to 1000 m numerous patches with degrading jellyfish were observed at the seabed. At 1200 m depth are some undegraded jellyfish corpses and little phytodetritus. At 1500 m a thick detrital layer (phytodetritus), believed to have been derived from the large phytoplankton production along the coast of Oman associated with SW monsoon upwelling events, covered the seabed, making observations extremely difficult. Some patches of decaying jellyfish were evident. At 2400 m depth large amounts of phytodetritus cover the seabed making it practically impossible to see any features of the seabed. Decaying jellyfish covered in white bacterial mats were seen, but they were not as common as in other areas. At 3200 m water depth a thin layer of jellyfish slime appeared to cover the whole sediment surface. The jelly detritus covers 95% of the seabed.

The amplitude decreases within the continental rise area are recorded on both the EM12 multibeam swath mapping backscatter map and the deep-towed CHIRP profile, overlying the same area. A layer of detritus covering this region may cause this reduction. However, the increase in towing height above 400 m within the continental rise area has to be also taken into consideration as an additional reason for amplitude decreases. It is not possible to distinguish these changes on the 3.5 kHz sediment profiler. Other ecosystems were not detected by any of the acoustic sources. The analysis of the amplitude profile from the EM12 multibeam swath mapping system and the deep-towed CHIRP suggest the combined use of both instruments might detect changes in benthic ecosystems in principal, if they result in distinct absolute amplitude changes and amplitude distributions. However, the acoustic response of the ecosystems encountered on the Oman margin during our study was too weak to confirm this.

Conclusions

Remote acoustic methods provide important means for interpreting sediment type and sedimentary processes in the marine environment. The EM12 multibeam swath mapping system is a very suitable system for seafloor characterization because of its relatively high spatial resolution and narrow beams (less then 1°), its large lateral coverage, and the simultaneous collection of topographic information. However, compared to the other acoustics sources that we used, it lacks sub-bottom information.

A comparison of a deep-towed CHIRP profiler with a traditional surface-towed sediment profiler shows the advantage of the deep-towed system which finds a confirmation in other authors' studies (Nordfjord et al., 2005). It provides high-resolution topography with sub-bottom information. Due to its constant, optimal 300 m towing height, it is not as affected by wave propagation effects such as diffractions and spherical divergence. This is why it is much better suited to detail seabed studies. However, the higher spatial resolution can also lead to misinterpretation of the results in areas with hummocky topography, because small-scale seabed undulations strongly increase scattering of the wave energy and this is more easily detected by the high spatial resolution of the deep-towed CHIRP system than by the conventional 3.5 kHz sediment profiler. Although 3.5 kHz systems have been used for many decades to characterize the seabed, we have shown that their potential to fulfill this task is far inferior to modern deep-towed chirp profilers. This difference is biggest for great water depth and it is primarily the result of their large footprint which causes a low lateral resolution and the effects of wave propagation artifacts in rough terrain. Furthermore, they require proper travel-time dependant amplitude correction before their amplitudes can be interpreted meaningfully. Therefore, a use of both EM12 multibeam swath mapping system and deep-towed CHIRP over the same area gives the best results at both regional and local scales. Previous studies proved the possibility of detecting large benthic ecosystem by (Milkert and Hühnerbach, 1997; De Mol et al., 2002; Huvenne et al., 2003). The analysis of the seabed reflection amplitude profiles from the EM12 multibeam swath mapping system and the deep-towed CHIRP suggests that the simultaneous use of both instruments should allow detecting changes in benthic ecosystems. However, it was not possible to corroborate this conclusion during our study offshore Oman because of the lack of significant ecosystems along the southern transect.

Acknowledgements

The manuscript benefited from helpful suggestions offered by two anonymous reviewers and the editor Peter Clift. The work was funded by the United Kingdom Natural Environment Research Council (Grant Number JGS 834 Scheherezade II). The Ministry of Defence supported the data evaluation through Joint Grant Scheme. We are grateful to Ian Rouse and Duncan Matthew for assistance with the deep-towed CHIRP. We thank the master of RRS Charles Darwin and his crew of Cruise 143.

References

Billett, D.S.M., Bett, B.J. and Wigham, B.D., 2003, Jelly lakes in the abyssal Arabian Sea – massive food falls? Tenth Deep Sea Biology Symposium, Coos Bay Oregon, 25–29 August 2003.

Briais, A., Sloan, H., Parson, L.M. and Murton, B.J., 2000, Accretionary processes in the axial valley of the Mid-Atlantic Ridge 27 degrees N-30 degrees N from TOBI side-scan sonar images, *Mar. Geophys. Res.* **21**(1–2), 87–119.

Cowls, S. and Fogg, B., 2000, How to choose a multibeam, *Int. Ocean Syst.* 4(4), 4–6.

De Mol, B., Van Rensbergen, P., Pillen, S., Van Herreweghe, K., Van Rooij, D., McDonnell, A., Huvenne, V., Ivanov, M., Swennen, R. and Henriet, J.P., 2002, Large deep-water coral banks in the Porcupine Basin southwest of Ireland, *Mar. Geol.* **188**(1–2), 193–231.

Gage, J.D. and Levin, L.A., 2000, Benthic processes in the deep Arabian Sea: introduction and overview, *Deep-Sea Res. Part I-Top. Stud. Oceanogr.* **47**(1–2), 1–7.

Gracia, E., Parson, L.M., Bideau, D. and Hekinian, R., 1998, Volcano-tectonic variability along segments of the Mid-Atlantic Ridge between Azores platform and Hayes fracture zone: evidence from submersible and high-resolution side-scan sonar data, in Mills, R.A. and Harrison, K. (eds.), Modern Ocean Floor Processes and the Geological Record, Geological Society of London, London, pp. 1–15.

Hammerstad, E., Asheim, S., Nilsen, K. and Bodholt, H., 1993, Advances in multibeam echo sounder technology Oceans '93, *Eng. Harmony Ocean IEEE* **1**, 1482–1487.

Heezen, B.C., Tharp, M. and Ewing, M., 1959, The floors of the oceans: 1 The North Atlantic, *Geol. Soc. Am. Special Paper* **65**, 122.

Huvenne, V.A.I., De Mol, B. and Henriet, J.P., 2003, A 3D seismic study of the morphology and spatial distribution of

buried coral banks in the Porcupine Basin SW of Ireland, *Mar. Geol.* **198**(1–2), 5–25.

Jacobs, C.J., 2003, SCHEREZADE II: Geological and biological surveys of the Arabian Sea and the continental slope of Oman, Cruise CD143, Cruise report no. 42, vol. 1, p. 79, Southampt. Oceanogr. Centre.

Keeton, J.A. and Searle, R.C., 1996, Analysis of Simrad EM12 multibeam bathymetry and acoustic backscatter data for seafloor mapping, exemplified at the Mid-Atlantic Ridge at 45 degrees N, *Mar. Geophys. Res.* **18**(6), 663–688.

Kim, G.Y., Kim, D.C., Park, S.C. and Lee, G.H., 2003, CHIRP (2–7) echo characters and geotechnical properties of surface sediments in the Ulleung Basin, the Easet Sea, *Geosci. J.* 3(4), 213–224.

Leblanc, L.R., Mayer, L., Rufino, M., Schock, S.G. and King, J., 1992, Marine sediment classification using the chirp sonar, *J. Acoust. Soc. Am.* **91**(1), 107–115.

Leetmaa, A., Quadfasel, D.R. and Wilson, D., 1982, Development of the flow field during the onset of the Somali current, 1979, *J. Phys. Oceanogr.* **12**(12), 1325–1342.

Meadows, A., Meadows, P.S., West, F.J.C. and Murray, J.M.H., 2000, Bioturbation, geochemistry and geotechnics of sediments affected by the oxygen minimum zone on the Oman continental slope and abyssal plain, Arabian Sea, *Deep-Sea Res. Part II-Top. Stud. Oceanogr.* **47**(1–2), 259–280.

Milkert, D. and Hühnerbach, V., 1997, Costal Environments, in Blondel, P. and Murton, B.J. (eds.), Handbook of Seafloor Sonar Imagery, Praxis Publishing Ltd. pp. 193–221.

Milliman, J.D., 1988, Correlation of 3.5-kHz acoustic penetration and deposition-erosion in the argentine basin – a note, *Deep-Sea Res. Part a-Oceanogr. Res. Papers* **35**(6), 919–937.

Nealon, J.W., Dillon, W.P., Danforth, W. and O'Brien, T.F., 2002, Deep towed chirp profiles of the Blake Ridge collapse structure collected abroad R/V Cape Hatteras in 1992 and 1995. U.S. Geological Survey Open-File Report 01–123, CD-ROM.

Nordfjord, S., Goff, J.A., Austin, J.A. Jr. and Sommerfield, C.K., 2005, Seismic geomorphology of buried channel systems on the New Jersey outer shelf: assessing past environmental conditions, *Mar. Geol.* **214**, 339–364.

Nouze, H., Sibuet, J.C., Savoye, B., Marsset, B. and Thomas, Y., 1997, Pasisar: performances of a high and very high resolution hybrid deep-towed seismic device, *Mar. Geophys. Res.* **19**(5), 379–395.

Richardson, M.D. and Briggs, K.B., 1993, On the use of acoustic impedance values to determine sediment properties, in Pace, N.G. and Langhore, D.N. (eds.), Acoustic Classification and Mapping of the Seabed, Proceedings of the Institute of Acoustics, Bath University Press, Bath UK, pp. 15–24.

Savoye, P.L., De Roeck, Y.H., Marsset, B., Lopes, L. and Herveou, J., 1995, PASISAR: a new tool for near-bottom very high-resolution profiling in the deep water, *First Break* **13**(6), 253–258.

Scheirer, D.S., Fornari, D.J., Humphris, S.E. and Lerner, S., 2000, High-resolution seafloor mapping using the DSL-120 sonar system: quantitative assessment of sidescan and phase-bathymetry data from the Lucky Strike segment of the Mid- Atlantic Ridge, *Mar. Geophys. Res.* **21**(1–2), 121–142.

Shimmield, G.B., Price, N.B. and Pederson, T.F., 1990, The influence of hydrography, bathymetry and productivity on sediment type and composition of the Oman margin and in the Northwest Arabian Sea, in Robertson, A.H.F., Searle, M.P. and Ries, A.C. (eds.), The Geology and Tectonics of the Oman Region, Geological Society Special publication, London, pp. 759–769.

Schurr Duncan, C., Goff, J.A., Austin, J.A. Jr. and Fulthorpe, C.S., 2000, Tracking the last sea-level cycle: seafloor morphology and shallow stratigraphy of the latest Quaternary New Jersey middle continental shelf, *Mar. Geol.* **170**, 395–421.

Schuur Duncan, C. and Goff, J.A., 2001, Relict iceberg keel marks on the New Jersey outer shelf, southern Hudson apron, *Geology* **29**(5), 411–414.

Thorne, P.D. and Pace, N.G., 1984, Acoustic studies of broadband scattering from a model rough-surface, *J. Acoust. Soc. Am.* **75**(1), 133–144.

Uchupi, E., Swift, S.A. and Ross, D.A., 2002, Morphology and late quaternary sedimentation in the Gulf of Oman Basin, *Mar. Geophys. Res.* **23**(2), 185–208.

Underwood, M.B. and Moor, F.G., 1995, Trenches and trench-slopes basin, in Busby, C.J. and Ingersoll, R.V. (eds.), Tectonics of Sedimentary Basin, Blackwell Science, Inc., Oxford, pp. 179–219.

Veeken, P.C.H. and Da Silva, M., 2004, Seismic inversion methods and some of their constraints, *First Break* **22**, 47–70.

Zitter, T.A.C., Huguen, C. and Woodside, J.M., 2005, Geology of mud volcanoes in the eastern Mediterranean from combined sidescan sonar and submersible surveys, *Deep-Sea Res. Part I-Oceanogr. Res. Papers* **52**(3), 457–475.